Preprints of the 21st IFAC World Congress (Virtual)
Berlin, Germany, July 12-17, 2020

Flatness-based Trajectory-tracking Control of Dielectric Elastomer Actuators

P. M. Scherer * **A. Irscheid** * **G. Rizzello** ** **J. Rudolph** *

* *Chair of Systems Theory and Control Engineering, Saarland University, 66123 Saarbrücken, Germany, (e-mail: {p.scherer, a.irscheid, j.rudolph}@lsr.uni-saarland.de)*
** *Intelligent Material Systems Lab, Saarland University, 66123 Saarbrücken, Germany, (e-mail: gianluca.rizzello@imsl.uni-saarland.de)*

Abstract: In recent years, actuators based on dielectric elastomers have become popular for both research and industrial applications. Due to their nonlinear behavior, they are typically used in on/off actuation. Established feedback control methods such as PID provide an effective and robust way to drive these actuators under constant setpoint requirements. However, such control methods exhibit poor trajectory tracking performance. This shortcoming is addressed in this work with a flatness-based nonlinear control design for a circular membrane actuator based on dielectric elastomers. By exploiting a nonlinear electro-mechanical model of the device, a tracking control law is designed in both feed-forward and feedback form. Moreover, it is shown how the flatness-based feed-forward control may be used to extend a conventional PID control to improve its tracking performance. The presented methods are validated and compared experimentally with a real actuator prototype. Tracking accuracy better than 10 μm along a 1 mm stroke trajectory (i. e. less than 1%) is shown. This result is a significant improvement over existing PID control laws.

Keywords: flatness, nonlinear control, feed-forward control, dielectric elastomer, dielectric elastomer actuator, membrane actuator

1. INTRODUCTION

A dielectric elastomer (DE) transducer consists of a thin polymer film sandwiched between two compliant electrodes. When a high voltage (usually several kilovolts) is applied, electrostatic forces attract the electrodes together. Due to the high mechanical compliance of the DE material, the polymer is compressed in the direction of the applied electric field. At the same time, the elastomer expands in the perpendicular direction, maintaining its volume (see Fig. 1).

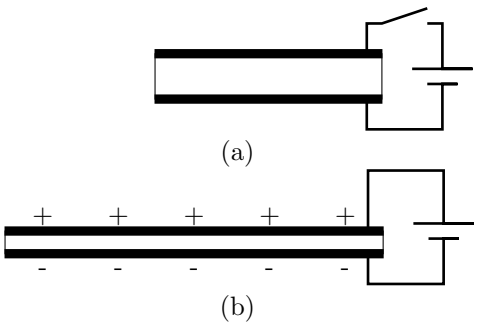

Fig. 1. Electro-mechanical actuation principle of a DE, (a) without high voltage and (b) with high voltage

This effect can be used in many different ways to realize a dielectric elastomer actuator (DEA). One example considered in this work and introduced by Hodgins et al. (2013) uses a circular DE membrane in combination with linear and bistable springs. This arrangement produces a significant strain that leads to a large out-of-plane stroke. The light weight, energy efficiency, and large strains of the DE material come at the expense of a complex nonlinear behavior due to hyperelasticity, electro-mechanical coupling, and viscoelasticity. Because of these effects, modeling and control of DEAs is challenging. As a result, most current DEA applications use the material in on/off mode only (see e. g. Giousouf and Kovacs (2013), Wang et al. (2018)). More sophisticated approaches that provide variable positioning include open-loop controllers (e. g. by Gu et al. (2015), Hau et al. (2017), and Zou and Gu (2019)) as well as closed-loop strategies (such as PID control by Xie et al. (2005), Druitt and Alici (2013), and Rizzello et al. (2015a), and further model-based designs by Hoffstadt and Maas (2017), Cao et al. (2018) and Zhang et al. (2019)).

Most of these linear and nonlinear controllers have been validated for position regulation tasks. In many applications, however, the DEA is required to perform accurate tracking of a specific trajectory. Examples include pumps (Wang et al. (2018)), loudspeakers (Heydt et al. (2006)), and soft robotics (Cao et al. (2018)). For these applications in particular, a model-based approach that accounts for nonlinear DE material effects is required.

This paper presents such an approach for a circular membrane DEA based on the mathematical model from Rizzello (2016). It will be shown that this model is differ-

entially flat and can be used to calculate a feed-forward control. Additionally, by exploiting the flatness property, a nonlinear tracking controller is designed. After developing the flatness-based controllers, they are validated experimentally in a trajectory tracking task for a DEA prototype. Results are compared with the existing robust PID approach from Rizzello et al. (2015a). It is also shown how this last method may be improved by introducing the flatness-based feed-forward term.

The present contribution is organized as follows. First, a phenomenological model of the DEA is presented in Section 2. In Section 3, the model properties are investigated and a flat output is introduced. The flatness property is then exploited to design controllers in both feed-forward and feedback forms. The details of their implementation and experimental results are shown in Section 4.

2. DEA MODEL

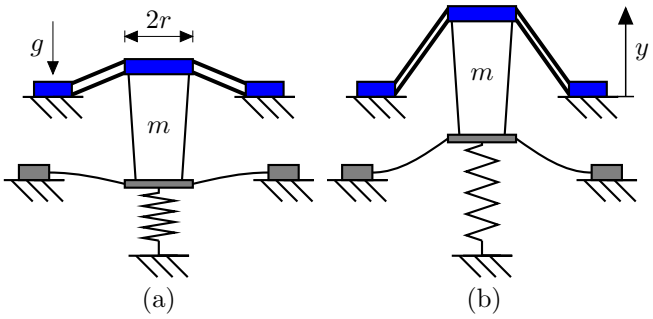

Fig. 2. Cross-sectional view of the circular DEA with linear spring, bistable spring and mass, (a) not actuated and (b) actuated

The circular membrane DEA takes on a truncated cone shape (see Fig. 2), with height increasing with applied voltage magnitude. Due to axial symmetry, a one-dimensional motion is assumed and may be described by considering the balance of momentum on the core of mass m in the y-direction

$$m\ddot{y} = -F_{\mathrm{P}}(y) - F_{\mathrm{DE}}(y, \dot{y}, v, \xi). \tag{1a}$$

The prestretching spring force and DE force derived in Rizzello (2016) are summarized in the following.

The force of the prestretch mechanism

$$F_{\mathrm{P}}(y) = k_{\mathrm{l}}(y - y_{\mathrm{l}}) + \sum_{b=0}^{P} k_{\mathrm{n},b}(y - y_{\mathrm{n},b})^b + mg \tag{1b}$$

is due to a linear spring with stiffness k_{l} and unstretched length y_{l}, a bistable spring modeled as a polynomial of degree P with parameters $k_{\mathrm{n},b}$ and $y_{\mathrm{n},b}$, $b = 0, 1, \ldots, P$, and the gravitational force. The force generated by the DE

$$F_{\mathrm{DE}}(y, \dot{y}, v, \xi) = \frac{V_0 y}{l_0^2 \lambda^2(y)} \Big(\sigma_{\mathrm{m}}(y) + \sigma_{\mathrm{e}}(y, v) + \sigma_{\mathrm{v}}(y, \dot{y}, \xi) \Big) \tag{1c}$$

depends on the volume V_0 of the DE as well as the initial radial length l_0. The function

$$\lambda(y) = \sqrt{1 + \left(\frac{y}{l_0}\right)^2} \tag{1d}$$

describes the principal stretch of the membrane in the radial direction depending on the position $y > 0$. Three physical effects contribute to the membrane force:

- The hyperelastic stress
$$\sigma_{\mathrm{m}}(y) = \sum_{i=1}^{3} \left[\beta_i \lambda^{2i}(y) - \gamma_i \lambda^{-2i}(y) \right], \tag{1e}$$
is modeled with an Ogden model of order 3 [1].
- The electro-mechanical coupling
$$\sigma_{\mathrm{e}}(y, v) = -\epsilon \left(\frac{\lambda(y) v}{z_0} \right)^2 \tag{1f}$$
is based on an ideal DE and is also called Maxwell stress. It depends on the initial thickness of the membrane z_0, its permittivity ϵ, and the applied voltage v.
- The viscoelastic stress
$$\sigma_{\mathrm{v}}(y, \dot{y}, \xi) = k_{\mathrm{v}} \left(\lambda(y) - 1 - \xi \right) + \eta_{\mathrm{p}} \dot{\lambda}(y, \dot{y}) \tag{1g}$$
with viscoelastic state ξ. The parameter k_{v} describes the stiffness of a spring within the equivalent rheological model of the DE. A stretch damping term enters linearly with the parameter η_{p}.

Completing the system equations is a first-order model of the viscoelastic state ξ with time constant τ_{v}:

$$\tau_{\mathrm{v}} \dot{\xi} = \lambda(y) - 1 - \xi. \tag{2}$$

3. CONTROLLER DESIGN

System equations (1)-(2) will now be used to design a nonlinear tracking control in open and closed-loop. The reference to track is planned in terms of the viscoelastic state ξ since it will be found to be a flat output of the system. As a result, this quantity has the following desirable properties [2]:

(I) Its reference trajectory may be chosen freely.
(II) The remaining system variables y and v can be expressed in terms of ξ and its derivatives.

Property (I) is true since no autonomous differential equation restricts ξ. Property (II) will be checked in the next Section for ξ and subsequently used to parameterize the input v for open-loop and closed-loop control.

3.1 Flatness-based parameterization

Solving (1d) and (2) for the position leads to the expression

$$y = l_0 \sqrt{\left(\tau_{\mathrm{v}} \dot{\xi} + \xi + 1 \right)^2 - 1} =: h_0(\xi, \dot{\xi}) \tag{3}$$

which depends on ξ and $\dot{\xi}$ only. As a consequence, higher order derivatives of y can be parameterized by ξ and its time derivatives according to

$$y^{(i)} = h_i \left(\xi, \ldots, \xi^{(i+1)} \right), \quad i = 0, 1, 2, \ldots \ . \tag{4}$$

Using (1a), (1c), and (1f), the remaining system variable v may be found to be

$$v = \pm \frac{l_0 z_0}{\sqrt{\epsilon}} \sqrt{\frac{m\ddot{y} + F_{\mathrm{P}}(y)}{V_0 y} + \frac{\sigma_{\mathrm{m}}(y) + \sigma_{\mathrm{v}}(y, \dot{y}, \xi)}{l_0^2 \lambda^2(y)}}, \tag{5}$$

[1] Further information about (1e) can be found in Rizzello (2016).
[2] For an introduction to differential flatness see Rothfuss et al. (1996)

from which only the positive root will be considered in the following. Substituting y, $\dot{y}$, and $\ddot{y}$ using (4) into (5) yields an expression for v in terms of ξ and its derivatives:

$$v = f\left(\xi, \dot{\xi}, \ddot{\xi}, \xi^{(3)}\right). \tag{6}$$

Since all system variables may be written in terms of ξ and its time derivatives, it is a flat output for (1)-(2).

3.2 Feed-forward control

One advantage of the flatness-based approach is that a feed-forward control may be calculated directly by substitution of a sufficiently smooth flat output reference trajectory in the corresponding expression for the system input. In this case for reference $t \mapsto \xi_\mathrm{r}(t)$, the feed-forward control using (6) is

$$v_\mathrm{FF} = f\left(\xi_\mathrm{r}, \dot{\xi}_\mathrm{r}, \ddot{\xi}_\mathrm{r}, \xi_\mathrm{r}^{(3)}\right). \tag{7}$$

The latter is the inverse of the model (1)-(2) with respect to the flat output ξ and thus no integration is required.

3.3 Linearizing tracking feedback controller

A closed-loop controller will be needed to compensate model errors and external disturbances. This controller may be designed by recognizing that the state $\boldsymbol{\psi}^\mathrm{T} = [\xi, \dot{\xi}, \ddot{\xi}]$ is a Brunovský state with respect to the input v. As a result, an auxiliary variable ν can be introduced as $\nu = \xi^{(3)}$ and viewed as a new virtual input (Rothfuss et al. (1996)). Given the error definition $e_\xi = \xi - \xi_\mathrm{r}$, a linear feedback can then be chosen as

$$\nu = \xi_\mathrm{r}^{(3)} - k_{\mathrm{D},2}\ddot{e}_\xi - k_{\mathrm{D},1}\dot{e}_\xi - k_\mathrm{P} e_\xi. \tag{8}$$

The parameters $k_{\mathrm{D},2}, k_{\mathrm{D},1}$, and k_P are selected in such a way that the eigenvalues of the differential equation of the error will have negative real parts. To ensure steady state accuracy, an integral part is also added according to

$$\bar{\nu} = \nu - k_\mathrm{I} \int_{t_0}^{t} e_\xi(s)\mathrm{d}s. \tag{9a}$$

The linearizing control law in terms of the physical system input is then

$$v_\mathrm{Lin.,I} = f\left(\xi, \dot{\xi}, \ddot{\xi}, \bar{\nu}\right). \tag{9b}$$

At this point it should be remarked that the feedforward (7) is also included in this tracking controller.

3.4 PID controller with flatness-based feed-forward

The above flatness-based control designs may likewise be used to improve the performance of existing controllers for this DEA. As an example, the robust PID controller with square root compensation from Rizzello et al. (2015a) is considered in the following. This approach, hereafter referred to simply as PID, is sketched briefly to demonstrate the integration of a flatness-based feed-forward term.

The PID control design frames the system (1)-(2) as a quasilinear parameter varying (qLPV) system with the state $\boldsymbol{x}$, the input transformation $u = v^2$, and the position y interpreted as the varying parameter. An error vector $\boldsymbol{e} = \boldsymbol{x} - \boldsymbol{x}_\mathrm{r}$ is defined, which obeys the differential equation

$$\dot{\boldsymbol{e}} = \bar{A}(y)\boldsymbol{e} + \bar{\boldsymbol{b}}(y)(u - w), \tag{10}$$

where $w = q(y, \boldsymbol{x}_\mathrm{r}, \dot{\boldsymbol{x}}_\mathrm{r})$ describes the influence of the reference trajectory $t \mapsto \boldsymbol{x}_\mathrm{r}(t)$ on the error. The parameters of the PID control

$$u_\mathrm{PID} = -\kappa_\mathrm{I} \int_0^t e_y(s)\mathrm{d}s - \kappa_\mathrm{P} e_y - \kappa_\mathrm{D}\dot{e}_y \tag{11}$$

with $e_y = y - y_\mathrm{r}$ are then chosen with an optimization method that includes the suppression of w.

While this strategy effectively treats w as a disturbance, knowledge of the reference trajectory may be used to reduce its influence. It can be shown that no equilibrium points of (10)-(11) exist with $e_y = 0$ unless

$$w|_{y=y_\mathrm{r}} = q(y_\mathrm{r}, \boldsymbol{x}_\mathrm{r}, \dot{\boldsymbol{x}}_\mathrm{r}) \tag{12}$$

is constant, which is not given for arbitrary reference trajectories. Therefore, a significant drawback of the proposed PID control (11) is its poor performance during transitions between stationary regimes, as can be seen in Section 4. To improve the trajectory tracking performance, the PID control may be extended according to

$$u = u_\mathrm{PID} + q(y_\mathrm{r}, \boldsymbol{x}_\mathrm{r}, \dot{\boldsymbol{x}}_\mathrm{r}) \tag{13}$$

in order to obtain an equilibrium point with $e_y = 0$ independent of the reference trajectory. It may be shown that the term $q(y_\mathrm{r}, \boldsymbol{x}_\mathrm{r}, \dot{\boldsymbol{x}}_\mathrm{r})$ coincides with v_FF^2, i. e. the flatness-based feed-forward control (7) and accounting for the input transformation. The corresponding physical input is then

$$v_\mathrm{PID+FF} = \sqrt{u_\mathrm{PID} + v_\mathrm{FF}^2}. \tag{14}$$

The practical performance of this augmented PID controller will be compared with the original PID controller (11) and the flatness-based linearizing controller (9) in the next section.

4. RESULTS

The experimental DEA setup uses a DE membrane made from SNES-18602-19RT5 from Parker Hannifin. A LK-G157 laser sensor measures the core position and an UltraVolt 4HVA24-P1 amplifier provides the actuating high voltage (see Fig. 3). For the implementation of the proposed model-based algorithms, the parameters introduced in Section 2 are needed. To this end, parameter identification is done as in Rizzello et al. (2015b) and Simone et al. (2018) where various voltage signals (step functions and sinusoids) are applied and the position y is measured. The MATLAB algorithm *fminsearch* is then used to fit the model parameters (see Table 1), with the exception of those for the prestretch system, to the experimental data. The springs are characterized by separate force-displacement measurements.

Further controller implementation details and experimental results are provided in the sequel.

4.1 Controller implementation and reference trajectories

For the implementation of the algorithms, system variables and their various time derivatives are needed. To this end, a laser sensor is used to measure the position y. By low-pass filtering and using the central difference quotient, a value for the velocity $\dot{y}$ is calculated out of these position measurements. Because ξ can not be measured

Table 1. Parameters of the model

Parameter	Value
z_0	$51\,\mu$m
l_0	12.5 mm
r	10 mm
m	5 g
ϵ	$2.26\,\epsilon_0$
β_1	$29.67\,\mathrm{MNm}^{-2}$
β_2	$-17.28\,\mathrm{MNm}^{-2}$
β_3	$3.19\,\mathrm{MNm}^{-2}$
γ_1	$53.69\,\mathrm{MNm}^{-2}$
γ_2	$-57.32\,\mathrm{MNm}^{-2}$
γ_3	$19.11\,\mathrm{MNm}^{-2}$
τ_v	1.44 s
k_v	$15.83\,\mathrm{kNm}^{-2}$
η_p	$1.12\,\mathrm{kNm}^{-2}\mathrm{s}$

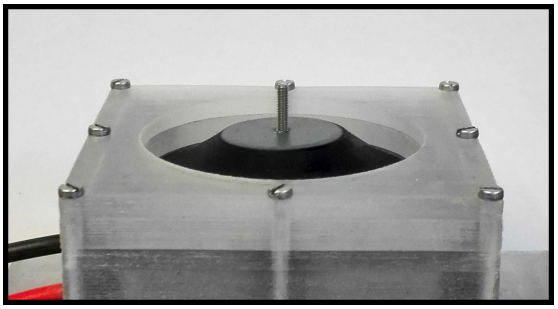

Fig. 3. Circular membrane DEA with prestretch system used for experiments

directly, a simulator is used to estimate it by numerically integrating (2). Once a value for ξ is known, (2) can be used to calculate $\dot{\xi}$. Thereafter, $\ddot{\xi}$ can be calculated by differentiating (2) with respect to time and using the values of y and $\dot{y}$ to calculate $\dot{\lambda}$.

The gains of the feedback linearizing controller (9) are chosen such that the eigenvalues of the error differential equation are as follows: $-45\,\mathrm{s}^{-1}$, $-40\,\mathrm{s}^{-1}$, $-30\,\mathrm{s}^{-1}$, $-3\,\mathrm{s}^{-1}$. The PID controller parameters $\kappa_\mathrm{P} = 1.1659\,(\mathrm{kV})^2\mathrm{mm}^{-1}$, $\kappa_\mathrm{I} = 44.5655\,(\mathrm{kV})^2\mathrm{mm}^{-1}\mathrm{s}^{-1}$, and $\kappa_\mathrm{D} = 0.0042\,(\mathrm{kV})^2\mathrm{mm}^{-1}\mathrm{s}$ are chosen for an exponential error decay rate for the qLPV system (10) of $\alpha = -20\,\mathrm{s}^{-1}$.

As seen in (7) and (8), a sufficiently smooth reference trajectory for ξ is needed for a continuous controller output. To this end, polynomial trajectories in time of degree 9 are planned to bring the system from one equilibrium point to another. By using the stationary solution of (2) as well as function the (1d), the corresponding values for ξ_r before and after the transition can be calculated from desired values for y_r. The remaining boundary conditions are set to zero. For the PID controller, the reference $t \mapsto y_\mathrm{r}(t)$ is calculated using (3).

Experimental results are shown next for planned trajectories with a 5 second transition time and various stroke magnitudes.

4.2 Feed-forward control

The resulting input voltages of the feed-forward controller (7) are shown in Fig. 4 (a). It is remarked how the voltage overshoots its final value to compensate the viscoelastic effects of the material. From Fig. 4 (b), it can be seen

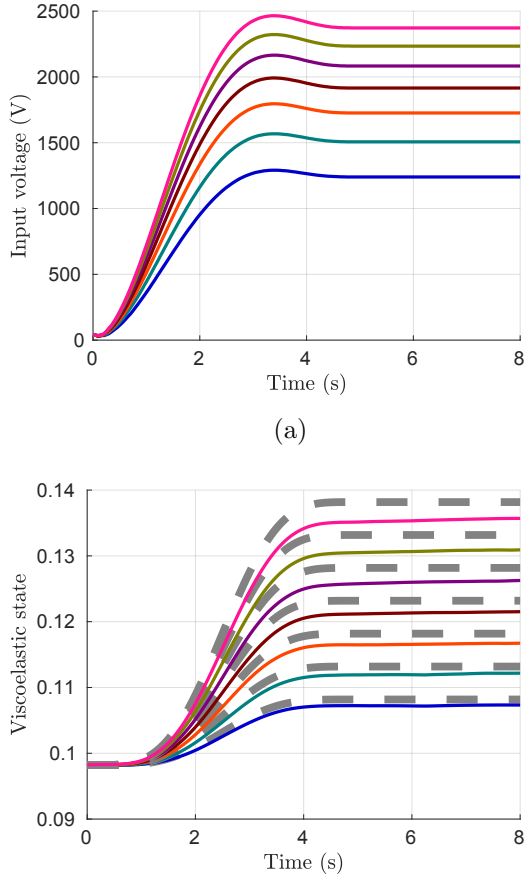

Fig. 4. Feed-forward control results for various stroke magnitudes. Measured and planned trajectories of the flat output ξ are shown as solid and dashed lines, respectively. Tracking and steady-state errors are due to model and parameter uncertainties.

that there is still a difference between the experimental viscoelastic response (solid lines) and its reference value (dashed lines). This means that some residual model and parameter uncertainties exist. This error in ξ may also be seen to increase with stroke magnitude. One explanation may be an unmodeled nonlinear effect due to the electrodes, which results into additional electro-mechanical hysteresis. Furthermore, a slowly decaying process is apparent in the response that continues to approach its reference value long after the transition interval. This effect may be attributed to further viscoelasticity on a larger time scale than considered in model (2). These effects motivate the need for a closed-loop controller.

4.3 Tracking feedback controllers

The flatness-based linearizing controller with integral action from (9) compensates these effects to yield excellent tracking performance as shown in Fig. 5. On the other hand, the PID control (11), while well regulating the final setpoint value, demonstrates poor performance during the trajectory transition stage in Fig. 6. Furthermore, this dynamic error increases with stroke magnitude. By adding the nonlinear feed-forward control from (14), PID control tracking accuracy is greatly improved (see Fig. 7). At a

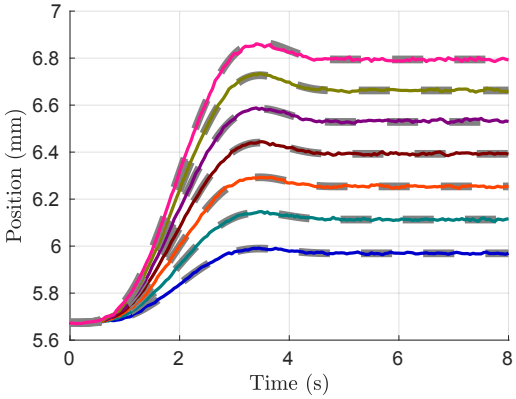

(a)

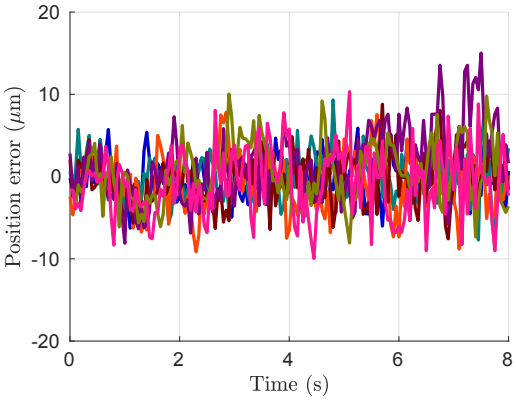

(b)

Fig. 5. Flatness-based linearizing control with integral action to increase the accuracy for transition and steady state

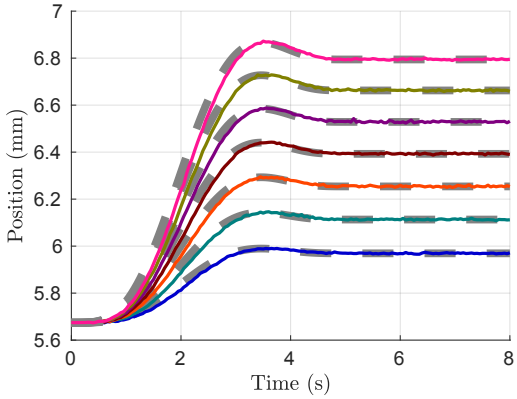

(a)

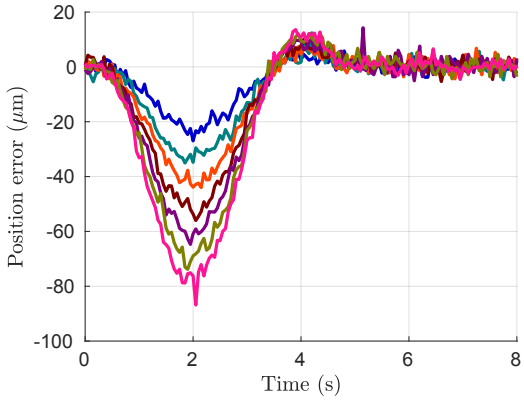

(b)

Fig. 6. PID controller for various strokes, demonstrates poor performance during transition

stroke of approximately 1 mm, tracking errors are smaller than $\pm 10\,\mu$m (except for random peaks of the sensor signal) and are comparable with the errors of the linearizing controller with integral action shown in Fig. 5.

5. CONCLUSION

A key aspect of this work was to demonstrate that an existing phenomenological model of the DEA is a flat system, whose flat output can be used to calculate feedforward and feedback controls. Experimental results validate this approach and demonstrate significantly better performance compared to a standard PID control for trajectory tracking. The results also show that the system model represents a good approximation of the complex DE material. The performance of the proposed controllers can be further improved by using additional viscoelastic states. This higher order system is still flat as shown in Appendix A.

Additionally, it should be remarked that the reference trajectory can be parameterized in terms of the position y instead of the viscoelastic state ξ if desired to prevent an overshoot in y. Since the flat output is not constrained to any differential equation, its value can be freely chosen. This means that if a sufficiently smooth trajectory for y is given, the required trajectory for ξ can be calculated, for example, by numerical integration of (2).

REFERENCES

Cao, J., Liang, W., Zhu, J., and Ren, Q. (2018). Control of a muscle-like soft actuator via a bioinspired approach. *Bioinspiration & biomimetics*, 13(6), 066005.

Druitt, C. and Alici, G. (2013). Intelligent control of electroactive polymer actuators based on fuzzy and neurofuzzy methodologies. *IEEE/ASME Transactions on Mechatronics*, 19(6), 1951–1962.

Giousouf, M. and Kovacs, G. (2013). Dielectric elastomer actuators used for pneumatic valve technology. *Smart Materials and Structures*, 22(10), 104010.

Gu, G., Gupta, U., Zhu, J., Zhu, L., and Zhu, X. (2015). Feedforward deformation control of a dielectric elastomer actuator based on a nonlinear dynamic model. *Applied Physics Letters*, 107(4), 042907.

Hau, S., Rizzello, G., Hodgins, M., York, A., and Seelecke, S. (2017). Design and control of a high-speed positioning system based on dielectric elastomer membrane actuators. *IEEE/ASME Transactions on mechatronics*, 22(3), 1259–1267.

Heydt, R., Kornbluh, R., Eckerle, J., and Pelrine, R. (2006). Sound radiation properties of dielectric elastomer electroactive polymer loudspeakers. In *Smart Structures and Materials 2006: Electroactive Poly-*

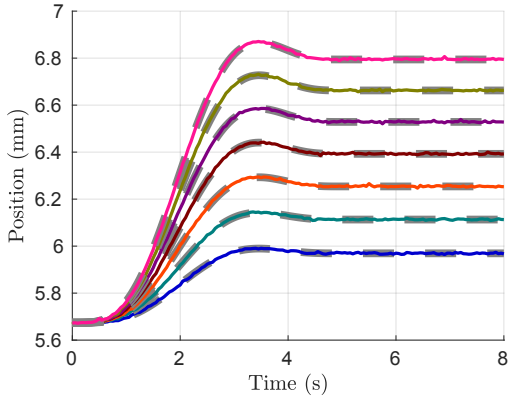

(a)

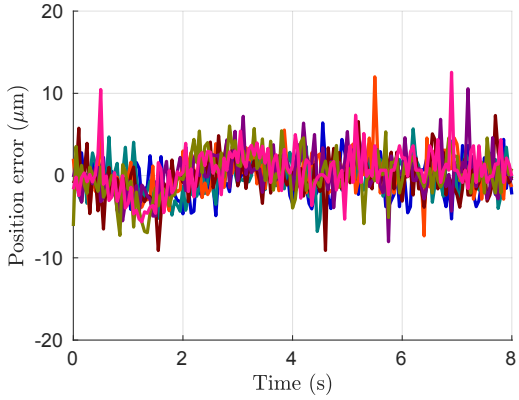

(b)

Fig. 7. PID controller with feed-forward control for improved transition performance

mer Actuators and Devices (EAPAD), volume 6168, 61681M. International Society for Optics and Photonics.

Hodgins, M., York, A., and Seelecke, S. (2013). Experimental comparison of bias elements for out-of-plane DEAP actuator system. *Smart Materials and Structures*, 22(9), 094016. doi:10.1088/0964-1726/22/9/094016.

Hoffstadt, T. and Maas, J. (2017). Adaptive sliding-mode position control for dielectric elastomer actuators. *IEEE/ASME Transactions on Mechatronics*, 22(5), 2241–2251.

Rizzello, G. (2016). *Modeling, Control and Self-Sensing of Dielectric Elastomer Actuators*. Ph.D. thesis, PhD thesis, Politecnico di Bari.

Rizzello, G., Naso, D., Turchiano, B., York, A., and Seelecke, S. (2015a). Robust lmi position regulation of a bistable dielectric electro-active polymer membrane. In *2015 54th IEEE Conference on Decision and Control (CDC)*, 84–90. IEEE.

Rizzello, G., Naso, D., York, A., and Seelecke, S. (2015b). Modeling, identification, and control of a dielectric electro-active polymer positioning system. *Control Systems Technology, IEEE Transactions on*, 23, 632 – 643. doi:10.1109/TCST.2014.2338356.

Rothfuss, R., Rudolph, J., and Zeitz, M. (1996). Flatness based control of a nonlinear chemical reactor model. *Automatica*, 32(10), 1433–1439.

Simone, F., Linnebach, P., Rizzello, G., and Seelecke, S. (2018). A finite element model of rigid body structures actuated by dielectric elastomer actuators. *Smart Materials and Structures*, 27(6), 065001.

Wang, Y., Li, Z., Qin, L., Caddy, G., Yap, C.H., and Zhu, J. (2018). Dielectric elastomer fluid pump of high pressure and large volume via synergistic snap-through. *Journal of Applied Mechanics*, 85(10), 101003.

Xie, S., Ramson, P., Graaf, D., Calius, E., and Anderson, I. (2005). An adaptive control system for dielectric elastomers. In *2005 IEEE International Conference on Industrial Technology*, 335–340. IEEE.

Zhang, M., Cao, X., Chen, X., Zhang, Z., Chen, Z., and Li, T. (2019). Model-based nonlinear control of the dielectric elastomer actuator with high robustness and precision. *Journal of Applied Mechanics*, 86(12).

Zou, J. and Gu, G. (2019). Feedforward control of the rate-dependent viscoelastic hysteresis nonlinearity in dielectric elastomer actuators. *IEEE Robotics and Automation Letters*, 4(3), 2340–2347.

Appendix A. VISCOELASTIC MODEL EXTENSION

If a DE material is used that shows a more pronounced viscoelastic behavior, an extended viscoelastic state $\boldsymbol{\xi}^{\mathrm{T}} = [\xi_1, \dots, \xi_M]$ may be introduced with the dynamics

$$\dot{\boldsymbol{\xi}} = A\boldsymbol{\xi} + \boldsymbol{b}u_\lambda \tag{A.1a}$$

and

$$A = \operatorname{diag}(-\tau_{\mathrm{v}j}^{-1}; j = 1, \dots, M) \tag{A.1b}$$

$$\boldsymbol{b}^{\mathrm{T}} = \left[\tau_{\mathrm{v}1}^{-1}, \dots, \tau_{\mathrm{v}M}^{-1}\right] \tag{A.1c}$$

as well as the new input $u_\lambda = \lambda(y) - 1$. The viscoelastic stress in (1) is then replaced by

$$\sigma_{\mathrm{v}}(y, \dot{y}, \boldsymbol{\xi}) = \sum_{j=1}^{M} k_{\mathrm{v}j}\big(\lambda(y) - 1 - \xi_j\big) + \eta_{\mathrm{p}}\dot{\lambda}(y, \dot{y}). \tag{A.2}$$

The natural question that arises is whether the extended DEA-model is flat. A key aspect for showing flatness for the case $M = 1$ in Subsection 3.1 is the fact that the position y can be parameterized by the viscoelastic state and its derivatives. With that in mind, proving flatness of the overall system with extended viscoelasticity reduces to finding a flat output of the viscoelastic subsystem (A.1).

The PBH controllability test for (A.1) shows that it is controllable if and only if all $\tau_{\mathrm{v}j}$, $j = 1, \dots, M$ are unique and nonzero, which is a well-known result for this particular system structure. If these conditions hold, it can be inferred that the (linear) model (A.1) is flat for arbitrary dimension M of the viscoelastic state with a corresponding flat output

$$\psi = \boldsymbol{t}^{\mathrm{T}}\boldsymbol{\xi}, \tag{A.3}$$

where $\boldsymbol{t}^{\mathrm{T}}$ is the last row of the inverse of the Kalman controllability matrix

$$\mathcal{C} = \left[\boldsymbol{b}, A\boldsymbol{b}, A^2\boldsymbol{b}, \dots, A^{M-1}\boldsymbol{b}\right]. \tag{A.4}$$

A consequence of the flatness of (A.1) is that the input u_λ and therefore the position y can both be parameterized by the flat output ψ, which implies flatness of the extended DEA-model. The flatness-based control strategies proposed in Section 3 can then be extended accordingly.